

MicroRNA-373-3p inhibits the proliferation and invasion of non-small-cell lung cancer cells by targeting the GAB2/PI3K/AKT pathway

XUNXIA ZHU, XIAOYU CHEN, XUELIN ZHANG, LITING ZHAO and XIAOYONG SHEN

Department of Thoracic Surgery, Huadong Hospital, Shanghai 200040, P.R. China

Received July 30, 2022; Accepted October 23, 2023

DOI: 10.3892/ol.2024.14353

Abstract. MicroRNAs (miRNAs) were previously demonstrated to be involved in the pathogenesis of non-small-cell lung cancer (NSCLC); however, the roles of certain miRNAs in NSCLC remain to be elucidated. The present study aimed to investigate the functions of screened miRNAs in NSCLC and the potential mechanisms. First, expression profiles of miRNAs were downloaded from the Gene Expression Omnibus (dataset no. GSE29248) and the differentially expressed miRNAs were analyzed by bioinformatics methods. Reverse transcription-quantitative PCR was used to validate the differential expression of miR-373 in clinical samples. The association between miR-373 expression levels and clinicopathological characteristics was also investigated. To further examine how miR-373 mediates the emergence of NSCLC, western blot, Cell Counting Kit-8, cell invasion and wound-healing assays, as well as apoptosis detection and a luciferase assay were used. The results indicated significant downregulation of miR-373 in NSCLC tissues and its low expression was closely associated with the degree of differentiation, clinical stage and tumor size, and was indicative of an unfavorable prognosis for patients with NSCLC. A functional study indicated that overexpression of miR-373 inhibited the proliferation, promoted apoptosis, and suppressed invasion and migration of NSCLC cells. Bioinformatics prediction and functional assays suggested that Grb-associated binding protein 2 (GAB2) was a direct target of miR-373. In addition, GAB2 was found to be significantly upregulated in NSCLC tissues, and clinically, miR-373 was negatively associated with GAB2. Furthermore, overexpression of GAB2 blocked the tumor suppressive effects of miR-373 on NSCLC cells. Mechanistically, miR-373 mimics were able to reduce the expression of GAB2 and subsequently decrease the phosphorylation level of AKT and mTOR protein. The present results indicate that miR-373

exerts its anti-tumor effects in NSCLC cells by targeting the GAB2/PI3K/AKT pathway, suggesting that miR-373 may be a potential therapeutic target in NSCLC.

Introduction

Currently, non-small cell lung cancer (NSCLC) is the leading cause of lung cancer-associated mortality, which accounts for up to 85% of all lung cancer cases (1). In spite of the improvement of the existing methods of diagnosis and treatment, as well as targeted therapy development, the recurrence and mortality rates remain high and the rate of 5-year survival is <20% (2-4). Therefore, it is crucial to deeply investigate the occurrence and mechanisms of NSCLC in order to explore novel therapeutic drug targets for early diagnosis and treatment, and to improve patient prognosis.

MicroRNAs (miRNAs) have a length of 20-25 nucleotides and regulate gene expression at the post-transcriptional stage by preventing transcription (5). In the past 10 years, it has become clear that miRNAs have critical roles in the regulation of tumor cell proliferation, as well as tumor invasion and metastasis (6,7). Numerous miRNAs have been determined to be ectopically expressed in NSCLC tissues and to promote the development or progression of the disease (6-11). For instance, miR-92a was found to be upregulated in NSCLC, and miR-92a overexpression led to the promotion of NSCLC tumor growth *in vivo* (12). miRNA-605 promotes cell proliferation, migration and invasion in NSCLC by directly targeting large tumor suppressor 2 (LATS2) (13). Furthermore, recent studies have indicated that miR-373 has important roles in human cancers, but the effect is controversial (14,15). A previous study reported that miR-373 may be associated with the progression of NSCLC (16). However, the biological role of miR-373 during the development of NSCLC requires further investigation.

The aim of the present study was to investigate the role of miR-373 in the regulation of NSCLC cell proliferation and invasion *in vitro* and the underlying molecular mechanism of this process. The current findings provided a new therapeutic strategy for clinical patients.

Materials and methods

Clinical specimens. From March 2019 to June 2020, 60 pairs of NSCLC tissues and adjacent non-tumor tissues were

Correspondence to: Professor Xiaoyong Shen, Department of Thoracic Surgery, Huadong Hospital, 221 Yanan West Road, Shanghai 200040, P.R. China
E-mail: xiaoyongshen77@163.com

Key words: non-small-cell lung cancer, miR-373, GAB2, AKT/mTOR signaling pathway

collected from 60 NSCLC patients who underwent lobectomy at the Department of Thoracic Surgery at Huadong Hospital (Shanghai, China). Patients were included when: i) They had primary NSCLC, excluding recurrence cases; ii) they did not receive radiotherapy, chemotherapy or other neoadjuvant treatment before surgery; iii) their diagnoses were confirmed by professional pathologists according to the NSCLC histopathological diagnostic criteria; and iv) had no history of other malignant tumors. All of the patients provided written informed consent prior to tissue collection. The clinicopathological data are presented in Table I. The present study was approved by the ethics committee of Huadong Hospital (Shanghai, China; approval no. 2019-0037). The adjacent tissue was 5 cm away from the edge of the tumour; all of the tissue samples were snap-frozen using liquid nitrogen, and then stored at -80°C until further analysis.

MiRNA expression profile data from Gene Expression Omnibus (GEO). The expression levels of miRNAs were assessed in NSCLC tissues and normal tissue samples from the GEO database (<https://www.ncbi.nlm.nih.gov/geo/query/acc.cgi?acc=GSE29248>). Differentially expressed miRNAs were identified using the R 'limma' package (version 4.2), which is a widely used tool that may be used to analyze data from any GEO series and significance analysis of microarray (SAM), to determine the differential expression of miRNAs among groups. miRNAs were considered to be differentially expressed according to the $P < 0.05$ threshold from the limma analysis and median false discovery rate < 0.05 from SAM. Data were visualized as heat maps using the online tool Morpheus (a web-based tool; <https://software.broadinstitute.org/morpheus/>).

Reverse transcription-quantitative (RT-q)PCR analyses. Total RNA from tumor tissues and transfected cells was isolated using the miRNeasy Mini kit (Qiagen GmbH). RNA concentrations were determined using the NanoDrop 2000 (Thermo Fisher Scientific, Inc.). To obtain complementary DNA (cDNA), 1.0 μg total RNA was added for reaction using the OneScript Plus Reverse Transcription Kit (GeneCopoeia) and the PrimeScript RT reagent Kit (Takara Biotechnology, Inc.) in a 20- μl total volume reaction according to the manufacturer's instructions. qPCR was performed using PowerTrack SYBR Green kit (Applied Biosystems; Thermo Fisher Scientific, Inc.) on a Bio-Rad CFX96 real-time PCR detection system (Bio-Rad Laboratories, Inc.) according to the manufacturer's instructions. PCR was conducted at 95°C for 10 min followed by 40 cycles of 95°C for 15 sec and 60°C for 60 sec. Primers for cDNA amplification were as follows: miR-21 forward, 5'-ATGCGCAACACCAGTCGATGG-3' and universal reverse, 5'-GCAGGGTCCGAGGTATTC-3'; miR-224 forward, 5'-CGCAGAAAATGGTGCCCTAGT-3'; miR-96 forward, 5'-CGCTAATCATGTGCAGTGCC-3'; miR-30a forward, 5'-GCAGCGCTTTCAGTCGGATGTT-3'; miR-126, forward, 5'-GCACGTCGTACCGTGAGTAAT-3'; miR-7 forward, 5'-CAGTGGAAAGACTAGTGATT-3'; miR-373 forward, 5'-CGAGAAGTGCTTCGATTTTG-3'; U6 forward, 5'-GCTTCGGCAGCACATATACTAAAAT-3' and reverse, 5'-CGCTTACGAATTTGCGTGTTCAT-3'; Grb-associated binding protein 2 (GAB2) forward, 5'-AGAAGTTGAGGC

GCTATGCC-3' and reverse, 5'-AAGGTGCGTTCACTG GTCTT-3'; GAPDH forward, 5'-TCAACGACCCCTTCATTG ACC-3' and reverse, 5'-CTTCCCGTTGATGACAAGCTTC-3'. miRNA was normalized to U6 and GAB2 was normalized to GAPDH. Data were analyzed by using the $2^{-\Delta\Delta\text{Ct}}$ method (17).

Cell lines and cell culture. The NSCLC cell lines (A549, H358 and H2170) were purchased from the American Type Culture Collection (ATCC) and the normal human bronchial epithelial cell line 16HBE was purchased from the Cell Bank of the Chinese Academy of Sciences. All cells were maintained in DMEM (Invitrogen; Thermo Fisher Scientific, Inc.) supplemented with 10% fetal bovine serum (FBS; Sigma-Aldrich; Merck KGaA) and specific antibiotics (100 U/ml penicillin and 0.1 mg/ml streptomycin) at 37°C in 95% air and 5% CO_2 .

Cell transfection. miR-373 mimics, mimics negative control (NC), inhibitor and inhibitor NC were synthesized by Genepharma (Shanghai, China). The sequences are as follows: MiR-373 mimics, 5'-GAAGUGCUCGUAUUUGGGU GU-3'; mimics NC, 5'-GCUUUAUAGAGUGCUAUUGC UU-3'; miR-373 inhibitor, 5'-ACACCCCAAAUCGAAGC ACUUC-3'; and inhibitor NC, 5'-AUUCUCAACCAAU CACGAAUA-3'. A549 and H358 cells were transfected using Lipofectamine[®] 2000 (Invitrogen; Thermo Fisher Scientific, Inc.) in accordance with the manufacturer's instructions with a GAB2-overexpression pcDNA3.1 plasmid (1 μg ; Invitrogen; Thermo Fisher Scientific, Inc.). As an NC, a pcDNA3.1 vector that was empty was utilized. After 48 h of transfection, the cells were harvested for the following experiments. The efficiency of overexpression or inhibition was verified by RT-qPCR and western blot.

Cell proliferation. A Cell Counting Kit (CCK)-8 assay (Dojindo Molecular Technologies, Inc.) was carried out in order to measure cell proliferation according to the manufacturer's instructions. In brief, A549 and H358 cells (2×10^4 cells) were seeded into 96-well plates and transfected with miR-373 mimics, mimics-NC or pcDNA-GAB2. The cells were then incubated for 1, 2 and 3 days at 37°C and 5% CO_2 in an incubator with 95% air and saturated humidity. Subsequently, 10 μl CCK-8 solution was added into each well and incubated for a further 2 h at 37°C , and the absorbance at 450 nm was measured using a microplate reader (Bio-Rad Laboratories, Inc.).

Cell apoptosis. The apoptotic rate was analyzed using an Annexin V-FITC/PI Apoptosis Detection kit (BD Biosciences) according to the manufacturer's protocol. In brief, following miR-373 mimics, mimics-NC or pcDNA-GAB2 transfection for 48 h, cells were digested with trypsin, centrifuged at $600 \times g$ for 5 min at 4°C and resuspended in 400 μl binding buffer. Subsequently, 5 μl Annexin V-fluorescein isothiocyanate (FITC) and 5 μl propidium iodide (PI) solution (cat. no. 556547; BD Pharmingen; BD Biosciences) was added and incubated in a dark room at room temperature for 20 min. The apoptotic cell ratio was then detected on a BD FACSCalibur flow cytometer (BD Biosciences) using FlowJo software (version 7.6.1; FlowJo LLC). The results showed healthy viable cells in the

Table I. Association between miR-373 and clinicopathological features of patients with non-small cell lung cancer.

Clinical parameters	Total (n=60)	MiR-373 expression		P-value
		High (n=35)	Low (n=25)	
Gender				0.4744
Male	38	23	15	
Female	22	22	10	
Age, years				0.8953
≥60	33	19	14	
<60	27	16	11	
Tumor size, cm				0.0455
≥5	42	21	21	
<5	18	14	4	
Smoking				0.5930
No	24	13	11	
Yes	36	22	14	
Differentiation degree				0.0395
Moderate	21	16	5	
Poor	39	19	20	
Clinical stage				0.0428
I-II	26	19	7	
III-IV	34	16	18	
Distant metastasis				0.1736
No	15	11	4	
Yes	45	24	21	
Lymph node involvement				0.0804
No	11	9	2	
Yes	49	26	23	

miR, microRNA.

lower left quadrant on the scatter plot as (FITC-/PI-). The lower right quadrant (Q3) represented the early-stage apoptotic cells as (FITC+/PI-). The upper right quadrant (Q2) represented late-stage apoptotic cells as (FITC+/PI+). The calculation was made as follows: Apoptotic rate=percentage of early-stage apoptotic cells (Q3) + percentage of late-stage apoptotic cells (Q2).

Caspase 3 activity assay. After treatment, total protein was extracted using RIPA buffer (cat. no. P0013B; Beyotime Institute of Biotechnology) and the protein concentration was evaluated using the bicinchoninic acid assay (cat. no. P0010S; Beyotime Institute of Biotechnology) according to the manufacturer's protocols. The caspase-3 activity assay was performed using a Caspase-3 colorimetric assay kit (cat. no. C1115; Beyotime Institute of Biotechnology) according to the manufacturer's protocol. The results were evaluated using a microplate reader (Bio-Rad Laboratories, Inc.) at 405 nm.

Western blot analysis. Total cellular proteins were lysed in RIPA lysis buffer (Beyotime Institute of Biotechnology) containing 2% protease inhibitor PMSF and the protein

concentration of each sample was evaluated with a bicinchoninic acid protein assay kit (Beyotime Institute of Biotechnology). Following separation by 10-12% SDS-PAGE, proteins were transferred onto a PVDF membrane (GE Healthcare; Cytiva). The membranes were blocked with a 5% skimmed milk solution in PBS with 0.05% Tween-20 overnight at 4°C, and then incubated with specific primary antibodies for 2 h at room temperature, including GAB2 (1:500 dilution; cat. no. ab32365), Bax (1:2,000; cat. no. ab32503), Bcl-2 (1:2,000; cat. no. ab32124), cleaved caspase 3 (1:2,000; cat. no. ab32042), E-cadherin (1:2,000; cat. no. ab40772), N-cadherin (1:1,500; cat. no. ab76011), Vimentin (1:1,000; cat. no. ab92547), Fibronectin (1:1,000; cat. no. ab2413), PI3K(p85) (1:1,000; cat. no. ab191606), mTOR (1:1,000; cat. no. ab2732), phosphorylated (p)-mTOR (1:1,000; cat. no. ab109268), Akt (1:1,000; cat. no. ab8805), p-Akt (1:2,000; cat. no. ab81283) and β-actin (1:1,000; cat. no. ab8227; all from Abcam). Subsequently, the membranes were incubated with the mouse anti-rabbit IgG-HRP antibody (1:1,000 dilution; cat. no. sc2537; Santa Cruz Biotechnology, Inc.) used as a secondary antibody for 60 min at room temperature. The proteins were visualized with an ECL kit (cat. no. 34580; Thermo Fisher Scientific,

Inc.). Semi-quantification was performed using ImageJ software (version 1.46; National Institutes of Health).

Transwell assay. At 24 h after transfection, 1.0×10^5 cells/200 μ l were added to the upper chambers of Transwell inserts with 8- μ m pores coated with Matrigel (Corning, Inc.). Furthermore, 600 μ l 10% FBS in DMEM was added to matched bottom chambers. After 48 h at 37°C, cells on the bottom filter surfaces were fixed for 15 min at room temperature with 4% paraformaldehyde (Beyotime Institute of Biotechnology) and stained for 10 min at room temperature with 0.1% crystal violet. Under an IX81 microscope (Olympus Corp.), images were acquired at a magnification of x100 and the number of invaded cells was calculated by analyzing five random fields per well.

Wound-healing assay. When cell confluence reached ~80%, a scratch wound was generated using the tip of 10- μ l pipette by making a straight line and the culture medium was replaced by DMEM supplemented with 1% FBS. Digital photographs were obtained at 0 and 48 h after scratching under a microscope at x100 magnification (Olympus IX81; Olympus Corp.) and the scratch area was measured using ImageJ software (version 1.46; National Institutes of Health).

Luciferase assays. The biological targets of miRNA targets were predicted using the algorithms TargetScan (https://www.targetscan.org/vert_80/) and microRNA.org (<http://www.microrna.org/>). The 3'-untranslated region (UTR) of human GAB2 was amplified as previously described (18) and cloned into pmirGLO (E1330; Promega Corp.) luciferase vector, named pGAB2-wild-type (WT). The human GAB2 mRNA was extracted from adjacent non-tumor lung tissues and reverse-transcribed to cDNA using a Reverse Transcription Kit with gDNA eraser kit (Takara Bio, Inc.). The mutant form of the 3'-UTR of GAB2 was also cloned into the pmirGLO vector to construct pGAB2-mutant (Mut) using the QuikChange Site-Directed Mutagenesis kit (Thermo Fisher Scientific, Inc.). To examine whether miR-373 directly target GAB2 mRNA, the reporter plasmids, WT-GAB2-PGL3 and Mut-GAB2-PGL3, were co-transfected with miR-373 mimics/inhibitor into 293T cells (7×10^4 ; ATCC) using Lipofectamine® 2000 according to the manufacturer's instructions. The relative firefly luciferase activity normalized to *Renilla* luciferase was measured 48 h after transfection by using the Dual-Light luminescent reporter gene assay (Applied Biosystems; Thermo Fisher Scientific, Inc.).

Statistical analysis. Statistical analysis was performed using SPSS software (version 16.0; SPSS Inc.). Values are expressed as the mean \pm standard deviation. An unpaired Student's t-test was used to perform comparisons of parameters between the two groups, while one-way analysis of variance followed by Tukey's post-hoc test was performed for comparing multiple groups. Differences in miR-373 expression and GAB2 gene expression between adjacent noncancerous tissues and cancer tissues were examined using a paired t-test. The correlation between miR-373 and clinicopathological features of patients with NSCLC was analyzed using the chi-square test; however, the variable 'lymph node involvement' was analyzed with Fisher's exact test. Survival rates were calculated using the

Kaplan-Meier method and comparisons were performed using the log-rank test. The correlation between the expression of miRNA and GAB2 was analyzed using Pearson's correlation analysis. $P < 0.05$ was considered to indicate statistical significance.

Results

miR-373 is downregulated in NSCLC tissues and cell lines. Using the GSE29248 microarray dataset, the differentially expressed miRNAs in NSCLC tissues and adjacent noncancerous tissues were first examined. As presented in Fig. 1A, 35 miRNAs were elevated and 25 miRNAs were downregulated in NSCLC. In addition, some of these miRNAs were confirmed by RT-qPCR in NSCLC tissues and adjacent noncancerous tissues in order to evaluate the validity of the *in silico* findings. According to the experimental results of the present study, miR-21, miR-224 and miR-96 were elevated, whereas miR-30a, miR-126 and miR-7 were downregulated (Fig. 1B), which was consistent with previous studies (19-24). Consistent with the array data, the results showed that miR-373 had the lowest expression and the most significant difference. Considerable evidence suggests that miR-373 is downregulated in multiple tumor tissues and acts as a tumor suppressor (14,15). Therefore, the subsequent research in the present study focused on this miRNA.

To confirm the downregulation of miR-373, its expression was then examined in 60 pairs of NSCLC and adjacent tissues by RT-qPCR. Compared to adjacent noncancerous tissues, miR-373 was found to be downregulated in NSCLC tissues (Fig. 1C). The association between miR-373 expression and survival outcomes among patients with NSCLC was then evaluated. According to the relative expression levels of miR-373-3p in 60 paired tumor and normal tissues, the patients were divided into two groups: High miR-373-3p group (miR-373-3p expression above the median value; $n=35$) and a low miR-373-3p group (miR-373-3p expression below the median value; $n=25$). The results indicated that miR-373 low expression was closely associated with the degree of differentiation, clinical stage and tumor size (Table I). Patients with NSCLC with low miR-373 expression had poorer overall survival than patients with high miR-373 expression (Fig. 1D). Subsequently, RT-qPCR was used to determine the expression of miR-373 in three NSCLC cell lines (A549, H358 and H2170) and a healthy human bronchial epithelial cell line (16HBE) in order to further determine whether miR-373 is downregulated in NSCLC cells. As indicated in Fig. 1E, the three NSCLC cell lines expressed miR-373 at a lower level than the 16HBE cells, indicating that miR-373 may have a role in the occurrence of NSCLC.

Overexpression of miR-373 suppresses cell proliferation and promotes apoptosis. To investigate the role of miR-373 in NSCLC, a gain-of-function analysis was performed by transfecting A549 and H358 cells with chemically synthesized miR-373 mimics. As presented in Fig. 2A, miR-373 levels were effectively enhanced after miR-373 mimics transfection in A549 and H358 cells. The results of the CCK-8 assay indicated that miR-373 mimics weakened the capacity of proliferation compared with that in the mimics NC group (Fig. 2B and C).

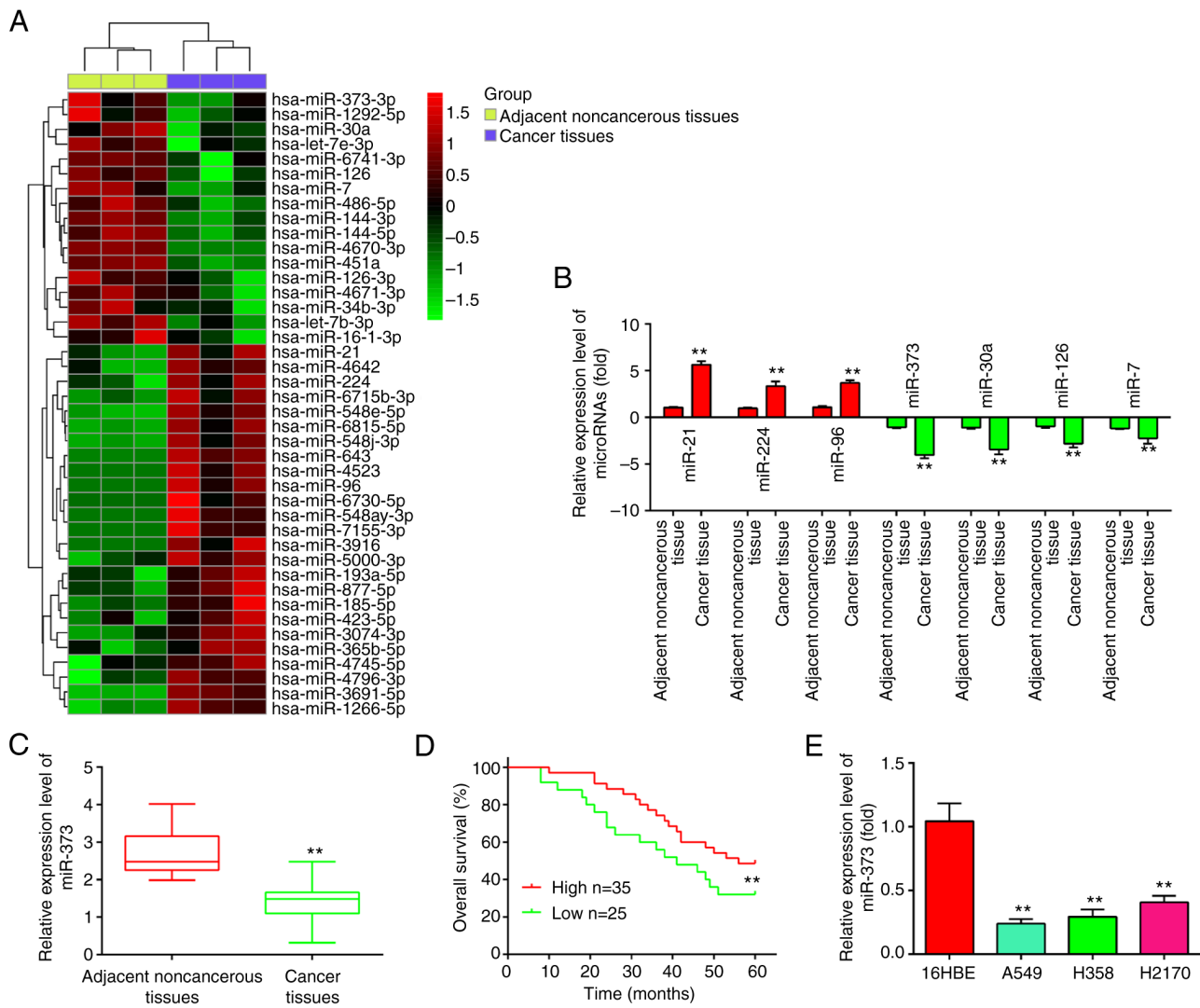


Figure 1. miR-373 is downregulated in NSCLC tissues and cell lines. (A) Differentially expressed miRNAs were analyzed between NSCLC cancer tissue and the adjacent normal tissue. The dataset was retrieved from Gene Expression Omnibus, with the accession number GSE29248. The color code in the heat map is linear and the expression levels of miRNAs that were upregulated are shown in green to red, whereas the miRNAs that were downregulated are shown in red to green. (B) The expression levels of miR-373, miR-21, miR-224 and miR-96, miR-30a, miR-126 and miR-7 were analyzed by RT-qPCR in NSCLC tissues and noncancerous tissues. (C) Relative expression of miR-373 was further analyzed by RT-qPCR in 60 pairs of NSCLC tissue and noncancerous tissues. (D) Kaplan-Meier overall survival curve for patients with NSCLC with miR-373-high and miR-373-low character. (E) Relative expression of miR-373 in three NSCLC cell lines (A549, H1299 and H358) and the normal human bronchial epithelial cell line 16HBE. Values are expressed as the mean \pm standard deviation. ** $P < 0.01$ vs. paired group/noncancerous tissues or 16HBE. miR-373, microRNA-373-3p; RT-qPCR, reverse transcription-quantitative PCR; NSCLC, non-small cell lung cancer.

Furthermore, the cell apoptosis rate was evidently increased in the miR-373 mimics compared with that in the mimics NC group (Fig. 2D). Consistently, miR-373 overexpression markedly increased the expression of cleaved-caspase-3 and Bax, and decreased the expression of Bcl2 in A549 and H358 cells compared with the levels in the mimics NC group (Fig. 2E). Collectively, these data indicate that overexpression of miR-373 suppressed cell proliferation and induced apoptosis in NSCLC cells.

Overexpression of miR-373 suppresses cell invasion and migration. Next, the migration and invasion ability of NSCLC cells were assessed by Transwell and wound-healing assays. The results of the Transwell assay indicated that miR-373 mimics led to a significant reduction in cell invasion compared to the mimics NC group (Fig. 3A and B). In the

wound-healing assay, it was shown that the cells' ability to metastasize was significantly weakened by miR-373 mimics compared with the mimics NC group (Fig. 3C and D). The influence of miR-373 on the protein markers of epithelial-mesenchymal transition (EMT) of A549 and H358 cells was then determined. The western blot results showed that the expression of E-cadherin, an epithelial marker, was markedly increased, while N-cadherin, Fibronectin and Vimentin, three mesenchymal markers, were significantly decreased in A549 and H358 cells after miR-373 mimics transfection (Fig. 3E). These results suggest that miR-373 regulates NSCLC cell invasion and migration via inhibiting the EMT process.

GAB2 is a direct target of miR-373. TargetScan and miRanda, two publicly accessible databases, were used to identify GAB2

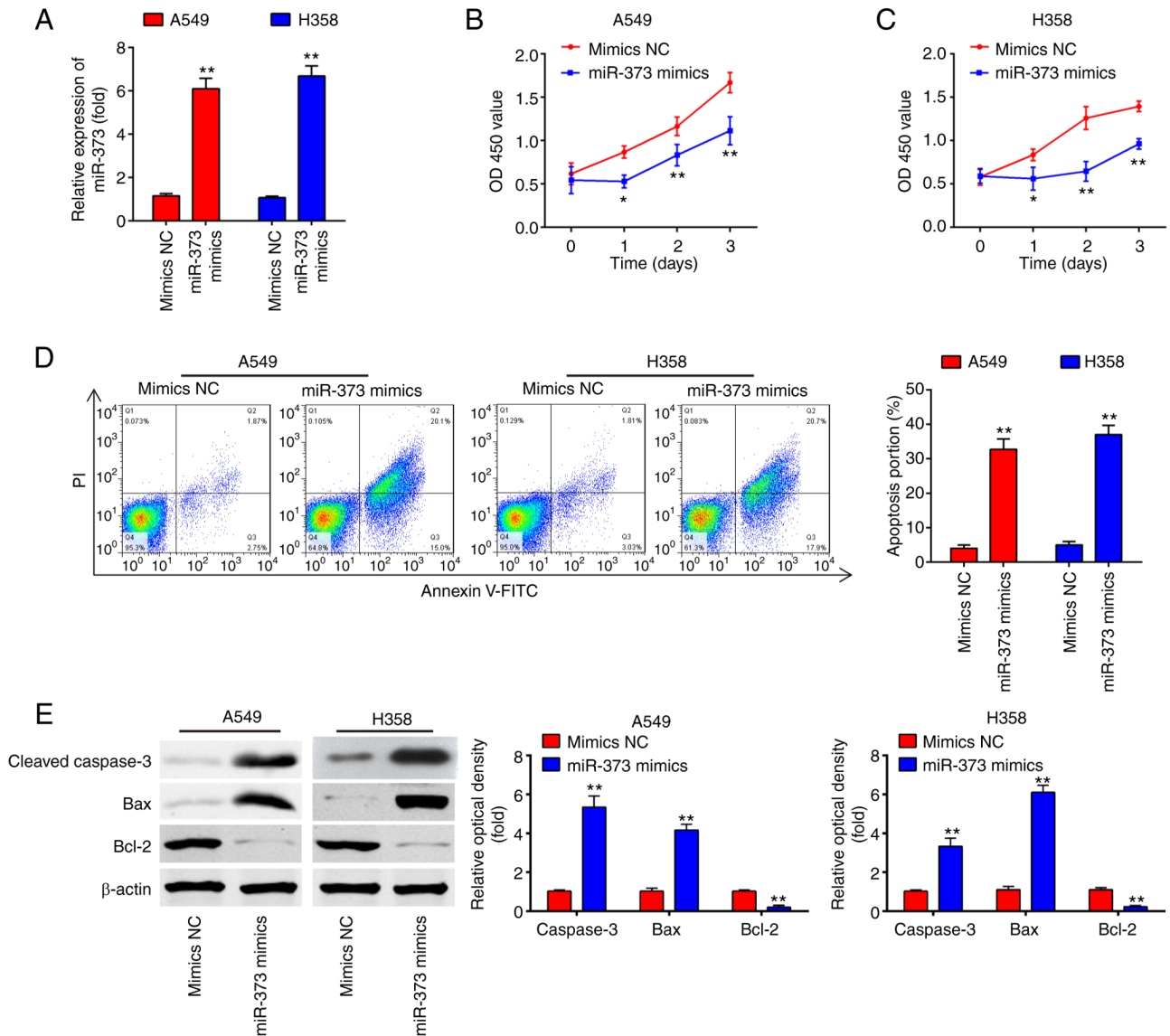


Figure 2. MiR-373 suppresses cell proliferation and promotes apoptosis. (A) Transfection of miR-373 mimics significantly increased the expression level of miR-373 in A549 and H358 cells. (B and C) Cell proliferation was measured with a Cell Counting Kit-8 assay after transfection in (B) A549 and (C) H358 cells. (D) The percentage of apoptotic A549 and H358 cells was evaluated by flow cytometry after transfection. (E) The expression levels of cleaved-caspase-3, Bcl-2 and Bax in A549 and H358 cells were detected by western blot after transfection. Values are expressed as the mean \pm standard deviation. * $P < 0.05$, ** $P < 0.01$ vs. mimics NC groups. MiR, microRNA; NC, negative control; PI, propidium iodide; OD450, optical density at 450 nm.

as a novel target of miR-373 (Fig. 4A). Previous research has shown that GAB2 is involved in a variety of carcinogenic activities, such as cellular growth, survival, proliferation and migration, through controlling the AKT pathway (25-27). To verify whether GAB2 is a direct target of miR-373, a luciferase reporter assay was performed. The results obtained with the dual-luciferase reporter assay system indicated that miR-373 mimics significantly suppressed the luciferase activity of the vector carrying the WT-GAB2 3'UTR, but not of that with the mutant 3'UTR, whereas knockdown of miR-373 led to the opposite result (Fig. 4B), indicating that miR-373 was able to bind to the GAB2 3'-UTR.

Subsequent experiments revealed that overexpression of miR-373 inhibited GAB2 expression at the mRNA and protein levels in A549 and H358 cells (Fig. 4C and D). Furthermore, RT-qPCR demonstrated that GAB2 expression levels were markedly increased in NSCLC cell lines and NSCLC tissues

as compared with 16HBE and adjacent noncancerous tissues, respectively (Fig. 4E and F). An obvious inverse correlation between GAB2 and miR-373 expression levels in NSCLC tissues was also observed (Fig. 4G). These results demonstrated that miR-373 was able to suppress the expression of GAB2 in NSCLC cells by directly targeting the GAB2 3'-UTR.

Overexpression of GAB2 attenuates the effects of miR-373 on cell proliferation and apoptosis. In order to determine whether miR-373 controls cell proliferation and apoptosis by targeting GAB2, pcDNA-GAB2 and miR-373 mimics were transfected into A549 and H358 cells. Following pcDNA-GAB2 transfection, GAB2 protein expression was markedly enhanced in A549 and H358 cells, as indicated in Fig. 5A. After transfection with miR-373 mimics, the expression level of GAB2 was significantly inhibited. However, this inhibitory effect was reversed by simultaneous GAB2

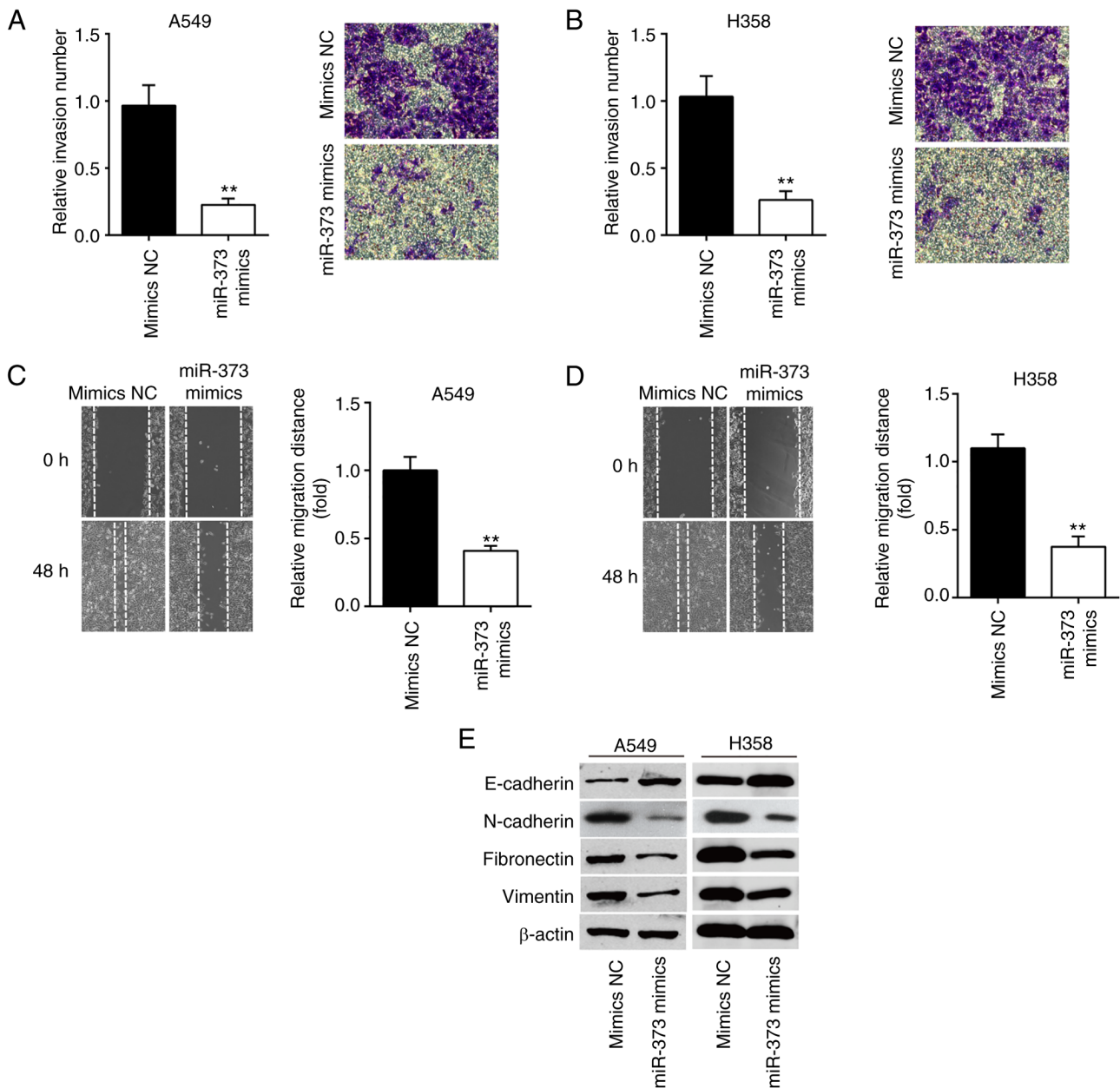


Figure 3. MiR-373 inhibits non-small cell lung cancer cell metastasis. (A and B) The invasion of (A) A549 and (B) H358 cells was measured by Transwell assay after transfection of miR-373 mimics (magnification, x200). (C and D) The migration of (C) A549 and (D) H358 cells was measured by wound-healing assay after transfection of miR-373 mimics (magnification, x200). (E) Expression levels of E-cadherin, N-cadherin, Fibronectin and Vimentin in H358 cells were detected by western blot after transfection of miR-373 mimics. Values are expressed as the mean \pm standard deviation. ** $P < 0.01$ vs. mimics NC. MiR, microRNA; NC, negative control.

overexpression. A549 and H358 cells transfected with miR-373 mimics had reduced cell proliferation compared with that in the mimics NC group, according to the results of a CCK-8 assay, whereas the inhibitory effect was efficiently attenuated by simultaneous overexpression of GAB2 (Fig. 5B and C). Furthermore, overexpression of GAB2 substantially reversed the stimulatory effects of miR-373 on caspase 3 activity and cell apoptosis in A549 and H358 cells (Fig. 5D-G). Together, these findings demonstrate that GAB2 contributes to the function of miR-373 in the proliferation and apoptosis of NSCLC cells.

Overexpression of GAB2 attenuates the inhibitory effects of miR-373 on the invasion and migration of NSCLC cells. Next,

it was investigated whether miR-373 regulates cell invasion and migration by targeting GAB2. As anticipated, miR-373 mimics-transfected A549 and H358 cell lines displayed decreased invasion activity when compared to the mimics NC group, while overexpression of GAB2 effectively reduced the inhibitory effect of miR-373 mimics (Fig. 6A-C). Similarly, overexpression of GAB2 abolished the effects of miR-373 mimics on migration (Fig. 6D-F). According to the above results, miR-373 mimics significantly raised E-cadherin expression, while significantly decreasing N-cadherin, Fibronectin and Vimentin levels, and simultaneous GAB2 overexpression significantly reversed these effects (Fig. 6G). These findings demonstrated that miR-373 inhibited cell invasion and migration by specifically targeting GAB2.

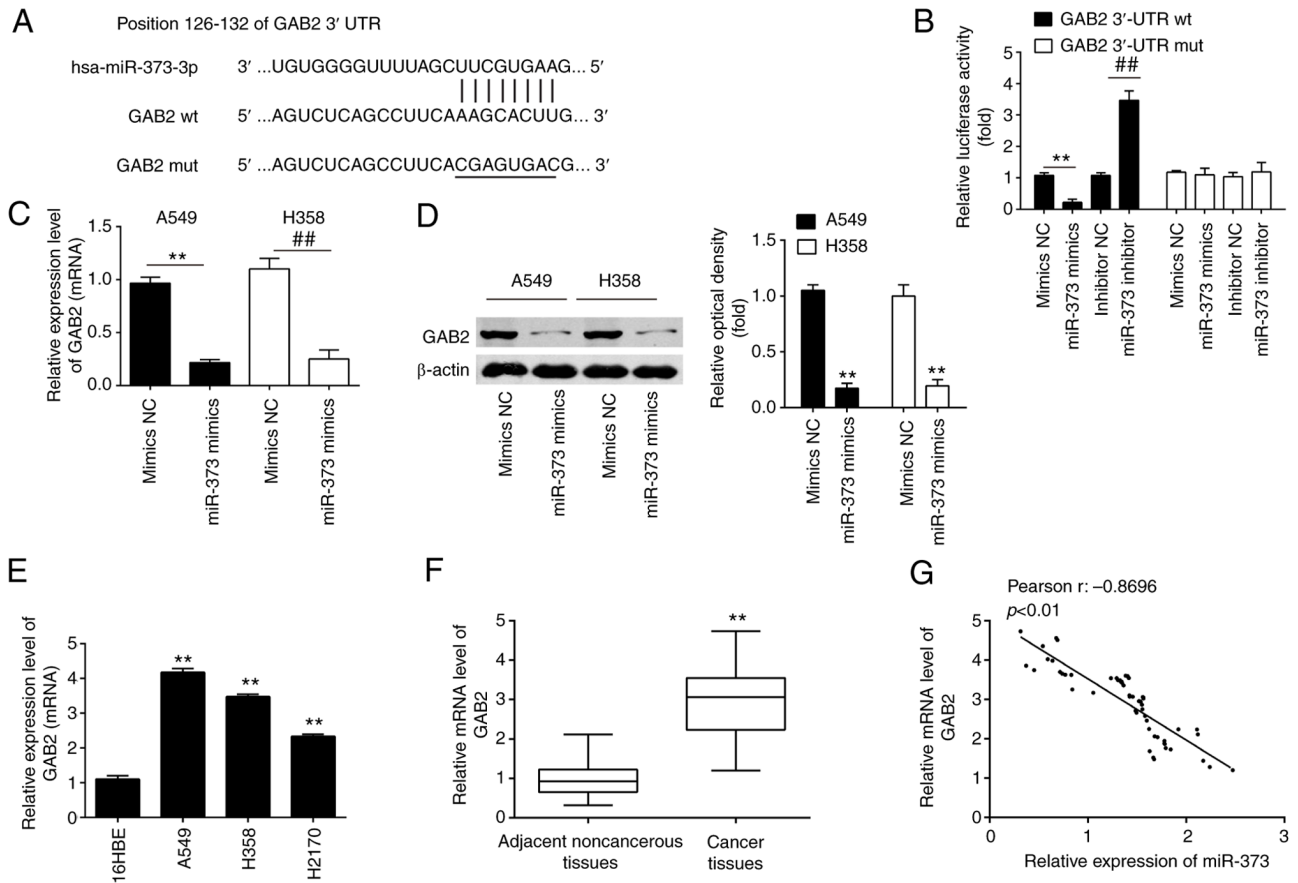


Figure 4. GAB2 is a direct target of miR-373 in NSCLC cells. (A) The predicted complementary sequences for miR-373 in the 3'-UTR of GAB2 and the mutations are shown in the seed region of miR-373. (B) miR-373 mimics and luciferase plasmids, which include WT GAB2 3'-UTR or Mut GAB2 3'-UTR, were co-transfected into 293T cells. The relative luciferase activity was determined. (C and D) GAB2 mRNA and protein expression levels were measured in (C) A549 and (D) H358 cells transfected with miR-373 mimics or inhibitor. Values are expressed as the mean \pm standard deviation. ** $P < 0.01$ vs. mimics-NC; ## $P < 0.01$ vs. inhibitor-NC. (E and F) Relative expression of GAB2 was further analyzed by RT-qPCR in (E) three NSCLC cell lines (A549, H1299 and H358) and (F) in 60 pairs of NSCLC tissue and noncancerous tissues. ** $P < 0.01$, compared with 16HBE cells or noncancerous tissues. (G) Pearson analysis for the correlation of GAB2 and miR-373 expression levels in patients with NSCLC ($r = -0.8696$; $P < 0.01$). MiR, microRNA; NC, negative control; GAB2, Grb-associated binding protein 2; RT-qPCR, reverse transcription-quantitative PCR; NSCLC, non-small cell lung cancer; WT, wild-type; Mut, mutant.

miR-373 suppresses the AKT/mTOR signaling pathway via downregulation of GAB2. GAB2 is an important oncogenic protein that affects the AKT/mTOR signaling pathway and regulates tumor cell proliferation, apoptosis and migration in various types of cancer, such as NSCLC and renal cell carcinoma (27-29). Thus, the following experiment was designed to study whether the miR-373/GAB2 regulatory axis affects the PI3K/AKT signaling pathway in NSCLC. The effects of miR-373 on proteins relevant to the AKT/mTOR signaling pathway were determined. It was shown that A549 and H358 cells with high expression of miR-373 had lower levels of GAB2, PI3K(p85), p-AKT and p-mTOR protein than those in the NC group, indicating that overexpression of miR-373 blocked AKT/mTOR signaling pathway activation. However, the inhibitory effect was reversed by overexpression of GAB2 (Fig. 7A-C). Collectively, these data suggest that miR-373 suppressed the AKT/mTOR signaling pathway via downregulation of GAB2.

Discussion

In the present study, it was found that miR-373 was downregulated in NSCLC tissues and cell lines, and closely associated

with the clinicopathological features and prognosis of patients with NSCLC. Furthermore, upregulation of miR-373 had a tumor suppressor effect in NSCLC cells by targeting GAB2/PI3K/AKT signaling. These findings implicate miR-373 as a potential therapeutic target for NSCLC.

Recent studies have indicated that miRNAs have a crucial role in tumor cell proliferation, apoptosis, invasion and migration (30,31). It has been reported that certain miRNAs, including miR-383 (32), miR-205 (33), miR-134 (34) and miR-132 (35), have important roles in regulating the proliferation and function of NSCLC cells. miR-383 overexpression inhibited proliferation, invasion and migration of A549 and H596 cells, and low tumorous miR-383 expression was significantly associated with poor prognosis of patients with NSCLC (32). It was previously reported that in lung cancer, miR-205 targeted Smad4 to promote cell growth *in vitro* and *in vivo* (33). Furthermore, miR-134 was observed to suppress NSCLC cell migration and invasion via regulating integrin beta 1 (34). To date, large-scale miRNA expression profile analysis has been carried out (36,37). In the present study, miRNA microarray profiling analysis was performed in the public dataset GSE29248, which was searched and downloaded

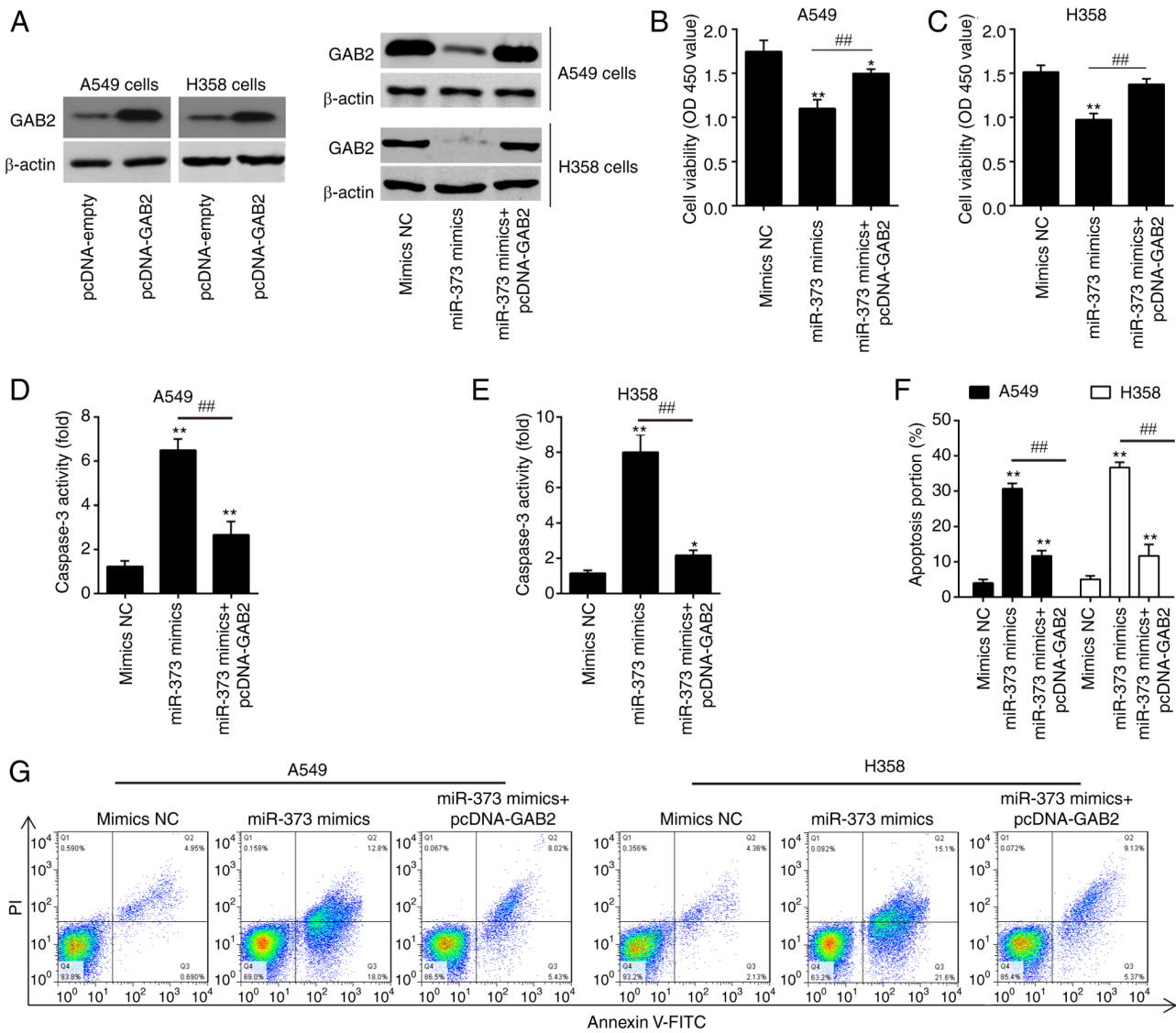


Figure 5. Overexpression of GAB2 reverses the anti-tumor effects of miR-373 mimics in non-small cell lung cancer cells. pcDNA-GAB2 was transfected into A549 and H358 cells, along with miR-373 mimics for 48 h and the cells were then harvested for further experiments. (A) The protein expression of GAB2 was measured by western blot. (B and C) Cell proliferation was measured by Cell Counting Kit-8 assay after transfection in (B) A549 and (C) H358 cells. (D and E) The activity of caspase 3 was measured by a commercial kit in (D) A549 and (E) H358 cells. (F and G) The percentage of apoptotic cells in each group and (E) representative flow cytometry dot plots. Values are expressed as the mean \pm standard deviation. * P <0.05, ** P <0.01 vs. mimics NC; ## P <0.01 vs. miR-373 mimics. MiR, microRNA; NC, negative control; GAB2, Grb-associated binding protein 2; OD450, optical density at 450 nm; PI, propidium iodide.

from the GEO database. A signature of miRNAs that was dysregulated in NSCLC tissues compared with that in normal samples of the GSE29248 dataset was identified, including those that have already been recognized by other studies: MiR-21, miR-224, miR-96, miR-30a, miR-126 and miR-7 (14-19). However, among these miRNAs, miR-373 showed the highest fold change in NSCLC samples compared to adjacent noncancerous tissues. miR-373, which has been shown to be aberrantly expressed in a variety of human cancers (14,15,38). However, the mechanism and function of miR-373 in NSCLC remain unclear. Therefore, miR-373 was selected for further study. In the present analysis, it was observed that miR-373 was significantly downregulated in NSCLC tissues and cell lines. Furthermore, miR-373 had a close relationship with the degree of differentiation, clinical stage, tumor size and prognosis of patients with NSCLC,

and it was indicated that miR-373 may be involved in the development of NSCLC.

To date, miR-373 has raised considerable interest in cancer research for its dual function as an oncogene and tumor suppressor (39,40). For instance, overexpression of miRNA-373-3p inhibited prostate cancer progression by targeting AKT1 (41). miR-373 overexpression decreased cell proliferation and invasion by targeting Ras-related protein Rab22a, a well-known oncoprotein in liver cancer cells (42). In cervical cancer, miR-373-3p targeted AKT1 to suppress cell growth *in vitro* and *in vivo* (43). Another previous study showed that the expression of miR-373 was decreased in NSCLC tissues and served as a tumor suppressor by targeting TFIIB-related factor 2 (44). As an oncogene, miR-373 promoted urinary bladder cancer cell proliferation, migration and invasion through upregulating epidermal growth

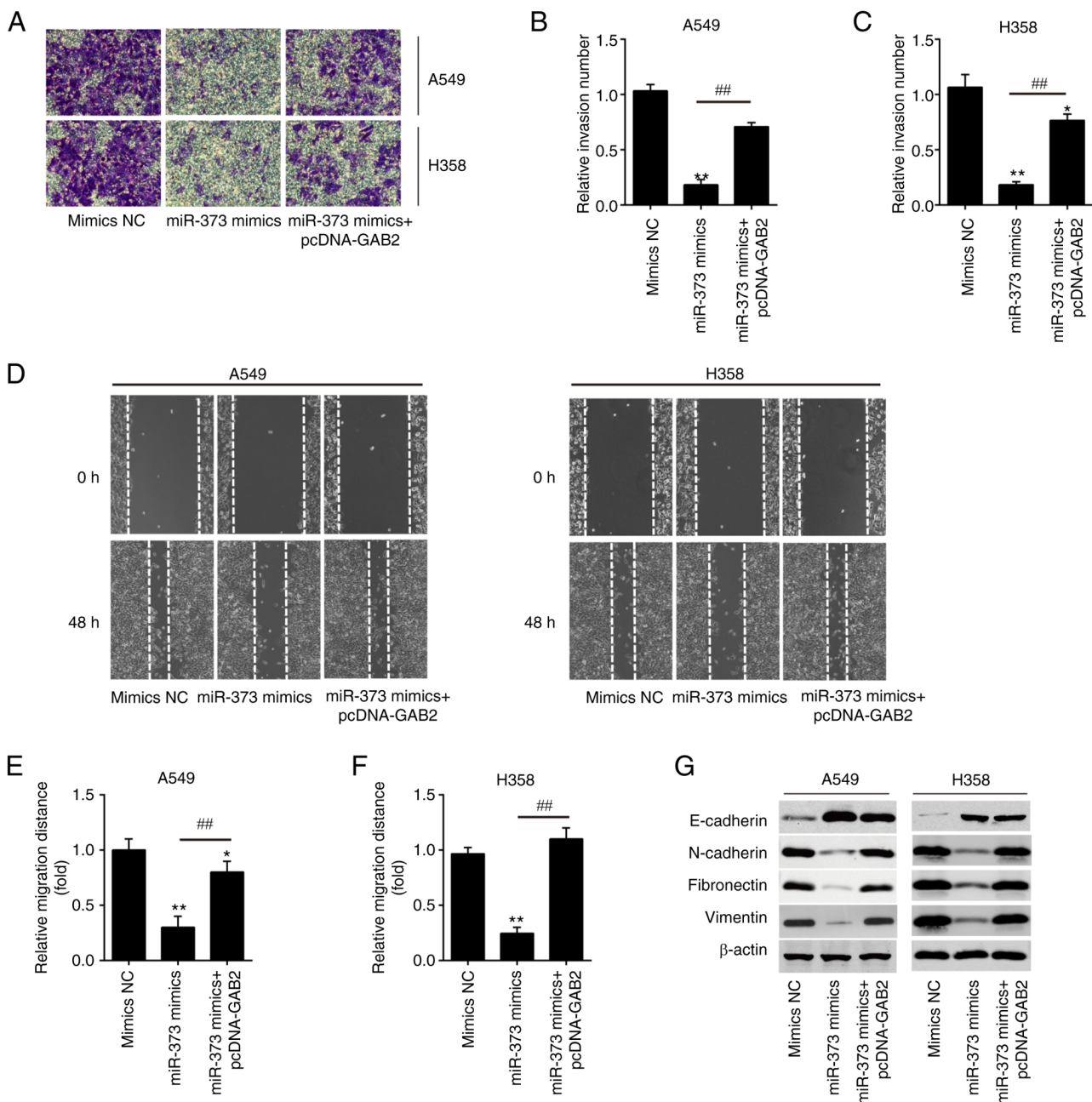


Figure 6. Overexpression of GAB2 is required for the miR-373-mediated suppression of migration and invasion in non-small cell lung cancer cells. pcDNA-GAB2 was transfected into A549 and H358 cells, along with miR-373 mimics, and the cells were then harvested for subsequent experiments. (A-C) The invasion of A549 and H358 cells was measured by Transwell assay after transfection. (A) Representative images and quantified results for (B) A549 and (C) H358 cells (magnification, x200). (D-F) The migration of A549 and H358 cells was measured by wound-healing assay after transfection. (D) Representative images and quantified results for (E) A549 and (F) H358 cells (magnification, x200). (G) The expression levels of E-cadherin, N-cadherin, Fibronectin and Vimentin in A549 and H358 cells were detected by western blot after transfection. Values are expressed as the mean \pm standard deviation. * $P < 0.05$, ** $P < 0.01$ vs. mimics NC, ## $P < 0.01$ vs. miR-373 mimics. MiR, microRNA; NC, negative control; GAB2, Grb-associated binding protein 2.

factor receptor (45). The present results confirmed the down-regulation of miR-373 expression in NSCLC and revealed that upregulation of miR-373 was able to suppress cell proliferation, promote apoptosis and inhibit migration and invasion in NSCLC cells. These findings suggested that miR-31-3p may act as a tumor suppressor of NSCLC. However, the underlying mechanism remained elusive.

After determining the biological functions of miR-373 in NSCLC, a functional analysis was subsequently performed to predict the molecular mechanisms underlying miR-373. According to a Bioinformatics analysis, GAB2 is directly

targeted by miR-373. GAB2, a scaffolding protein, mediates interactions with various signaling pathways and is involved in the regulation of tumor cell proliferation, apoptosis and migration (46,47). For instance, GAB2 promoted tumor cell migration and invasion, and enhanced tumor growth and metastasis *in vivo* in melanoma (48). GAB2 was overexpressed in breast cancer cell lines and primary tumors, and its overexpression increased the proliferative capacity of mammary epithelial cells (49). Regarding NSCLC, GAB2 disruption impaired the migration of NSCLC cell lines H1975 and H1299 (50). In the present study, it was indicated that GAB2 was highly

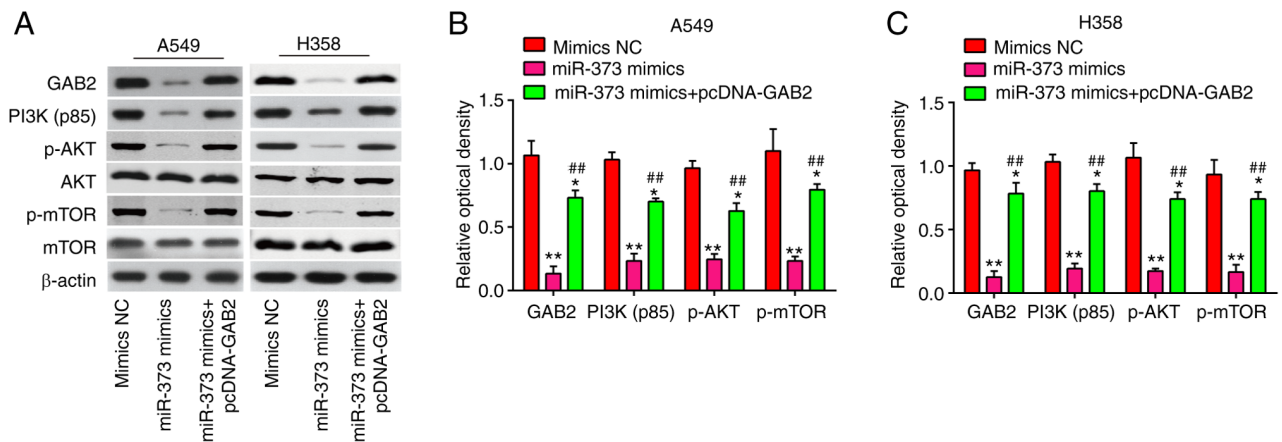


Figure 7. MiR-373 regulates the GAB2-mediated PI3K/AKT signaling pathway. pcDNA-GAB2 was transfected into A549 and H358 cells, along with miR-373 mimics, and the cells were then harvested for western blot. (A) Protein levels of GAB2, PI3K(p85), p-AKT, AKT, p-mTOR and mTOR were detected by western blot analysis. Bands for (B) A549 and (C) H358 cells were semi-quantitatively analyzed by using ImageJ software (version 1.46), normalized to β -actin density. Values are expressed as the mean \pm standard deviation. * $P < 0.05$, ** $P < 0.01$ vs. mimics NC, ## $P < 0.01$ vs. miR-373 mimics. MiR, microRNA; NC, negative control; GAB2, Grb-associated binding protein 2; p-AKT, phosphorylated AKT.

expressed in NSCLC tissues and cell lines, and negatively correlated with the level of miR-373 in NSCLC tissues. These observations demonstrate that GAB2 can promote migration and invasion, which counteract the role of miR-373. To further explore whether the anti-tumor effect of miR-373 is mediated by GAB2, rescue experiments were performed by introducing GAB2. It was found that manipulation of GAB2 could abrogate the regulative role of miR-373 in NSCLC cells.

Multiple cellular signaling pathways were reported to be dysregulated in NSCLC, such as the Ras/mTOR pathway and PI3K-AKT pathway. In the present study, GAB2 was identified as a functional target of miR-373 in the regulation of NSCLC cell proliferation, invasion and migration. It is known that GAB2 has three tyrosine residues, one of which specifically binds to the P85 subunit in PI3K, and this interaction is important for the activation of PI3K (51,52). The PI3K/Akt pathway has significant regulatory roles in cell proliferation, apoptosis and invasion (53). Furthermore, the PI3K/Akt pathway is aberrantly activated in malignant tumors including NSCLC, leading to upregulated growth (54). Therefore, PI3K/Akt pathway was selected for further study. The present results demonstrated that the phosphorylation status of AKT and mTOR and the expression of PI3K(p85) were significantly decreased when miR-373 was overexpressed, but it was reactivated by GAB2 upregulation.

Of note, the present study had certain limitations. First, miR-373 is not the sole anti-tumor element in NSCLC. Similarly, GAB2 is the only target gene of miR-373; there are other genes as well. The results of the present study suggested that the GAB2/PI3K/AKT signaling pathway may be one of the main mechanisms through which miR-373 exerts its tumor suppressive role in NSCLC. However, there may be other mechanisms by which miR-373 exerts its tumor suppressive role in NSCLC and a study reported that miR-373 targeted the TGF- β -R2/SMAD pathway to suppress cell proliferation and migration in prostate cancer (55). Another study also demonstrated that miR-373 targeted LATS2 and oxidation resistance 1 to regulate the Hippo and the p53 signaling pathway to promote the development of esophageal squamous cell carcinoma (56); thus, further investigation is required. In addition, more samples and further studies

are needed to unravel the relationship between miR-373-3p and the clinicopathological features of patients with NSCLC.

In conclusion, the present study demonstrated that miR-373 is a crucial regulator in the tumorigenesis of NSCLC, which is at least partially associated with GAB2-mediated PI3K/Akt pathway activation. In the future, they will be verified on a large number of clinical samples to evaluate the utility of miR-373-3p as a diagnostic marker or therapeutic target.

Acknowledgements

Not applicable.

Funding

This study was supported by the Clinical Science and Technology Innovation Project of Shanghai Hospital Development Center (grant no. SHDC22021218).

Availability of data and materials

The datasets used and/or analyzed during the current study are available from the corresponding author on reasonable request.

Authors' contributions

XXZ, XYC and LXZ performed the experiments, contributed to data analysis and wrote the manuscript. XXZ, XYC and LTZ analyzed the data. YYS conceptualized and designed the study, and contributed to data analysis and experimental materials. XXZ and YYS confirm the authenticity of all the raw data. All authors have read and approved the final manuscript.

Ethics approval and consent to participate

The present study was approved by the ethics committee of Huadong Hospital (Shanghai, China). All patients provided written informed consent to participate in the study.

Patient consent for publication

Not applicable.

Competing interests

The authors declare that they have no competing interests.

References

- Chen P, Li Y, Liu R, Xie Y, Jin Y, Wang M, Yu Z, Wang W and Luo X: Non-small cell lung cancer-derived exosomes promote proliferation, phagocytosis, and secretion of microglia via exosomal microRNA in the metastatic microenvironment. *Transl Oncol* 27: 101594, 2023.
- Mercier O, Fadel E, de Perrot M, Mussot S, Stella F, Chapelier A and Dartevelle P: Surgical treatment of solitary adrenal metastasis from non-small cell lung cancer. *J Thorac Cardiovasc Surg* 130: 136-140, 2005.
- Hirsch FR, Scagliotti GV, Mulshine JL, Kwon R, Curran WJ Jr, Wu YL and Paz-Ares L: Lung cancer: Current therapies and new targeted treatments. *Lancet* 389: 299-311, 2017.
- Giovannetti E, Toffalorio F, De Pas T and Peters GJ: Pharmacogenetics of conventional chemotherapy in non-small-cell lung cancer: A changing landscape? *Pharmacogenomics* 13: 1073-1086, 2012.
- Shi L, Zhu W, Huang Y, Zhuo L, Wang S, Chen S, Zhang B and Ke B: Cancer-associated fibroblast-derived exosomal microRNA-20a suppresses the PTEN/PI3K-AKT pathway to promote the progression and chemoresistance of non-small cell lung cancer. *Clin Transl Med* 12: e989, 2022.
- Han B, Molins L, He Y, Viñolas N, Sánchez-Lorente D, Boada M, Guirao A, Díaz T, Martínez D, Ramirez J, *et al*: Characterization of the MicroRNA Cargo of Extracellular Vesicles Isolated from a Pulmonary Tumor-Draining Vein Identifies miR-203a-3p as a relapse biomarker for resected non-small cell lung cancer. *Int J Mol Sci* 23: 7138, 2022.
- Yan X, Wang T and Wang J: Circ_0016760 Acts as a Sponge of MicroRNA-4295 to Enhance E2F transcription factor 3 expression and facilitates cell proliferation and glycolysis in non-small cell lung cancer. *Cancer Biother Radiopharm* 37: 147-158, 2022.
- Gong J, Shen Y, Jiang F, Wang Y, Chu L, Sun J, Shen P and Chen M: MicroRNA-20a promotes non-small cell lung cancer proliferation by upregulating PD-L1 by targeting PTEN. *Oncol Lett* 23: 148, 2022.
- MicroRNA-211 promotes non-small-cell lung cancer proliferation and invasion by targeting MxA [Retraction]. *Onco Targets Ther* 15: 1387-1388, 2022.
- Wei J, Meng G, Wu J, Wang Y, Zhang Q, Dong T, Bao J, Wang C and Zhang J: MicroRNA-326 impairs chemotherapy resistance in non small cell lung cancer by suppressing histone deacetylase SIRT1-mediated HIF1 α and elevating VEGFA. *Bioengineered* 13: 5685-5699, 2022.
- Fang X, Shi H and Sun F: The microRNA-520a-3p inhibits invasion and metastasis by targeting NF-kappaB signaling pathway in non-small cell lung cancer. *Clin Transl Oncol* 24: 1569-1579, 2022.
- Lu C, Shan Z, Hong J and Yang L: MicroRNA-92a promotes epithelial-mesenchymal transition through activation of PTEN/PI3K/AKT signaling pathway in non-small cell lung cancer metastasis. *Int J Oncol* 51: 235-244, 2017.
- Ye Y, Zhuang J, Wang G, He S, Ni J, Xia W and Wang J: microRNA-605 promotes cell proliferation, migration and invasion in non-small cell lung cancer by directly targeting LATS2. *Exp Ther Med* 24: 488, 2022.
- Eyking A, Reis H, Frank M, Gerken G, Schmid KW and Cario E: MiR-205 and MiR-373 are associated with aggressive human mucinous colorectal cancer. *PLoS One* 11: e0156871, 2016.
- Zhang Y, Zhao FJ, Chen LL, Wang LQ, Nephew KP, Wu YL and Zhang S: MiR-373 targeting of the Rab22a oncogene suppresses tumor invasion and metastasis in ovarian cancer. *Oncotarget* 5: 12291-12303, 2014.
- Seol HS, Akiyama Y, Shimada S, Lee HJ, Kim TI, Chun SM, Singh SR and Jang SJ: Epigenetic silencing of microRNA-373 to epithelial-mesenchymal transition in non-small cell lung cancer through IRAK2 and LAMP1 axes. *Cancer Lett* 353: 232-241, 2014.
- Livak KJ and Schmittgen TD: Analysis of relative gene expression data using real-time quantitative PCR and the 2(-Delta Delta C(T)) Method. *Methods* 25: 402-408, 2001.
- Li J, Xu J, Yan X, Jin K, Li W and Zhang R: MicroRNA-485 plays tumour-suppressive roles in colorectal cancer by directly targeting GAB2. *Oncol Rep* 40: 554-564, 2022.
- Wei J, Gao W, Zhu CJ, Liu YQ, Mei Z, Cheng T and Shu YQ: Identification of plasma microRNA-21 as a biomarker for early detection and chemosensitivity of non-small cell lung cancer. *Chin J Cancer* 30: 407-414, 2011.
- Cui R, Meng W, Sun HL, Kim T, Ye Z, Fassan M, Jeon YJ, Li B, Vicentini C, Peng Y, *et al*: MicroRNA-224 promotes tumor progression in non-small cell lung cancer. *Proc Natl Acad Sci USA* 112: E4288-E4297, 2015.
- Ma L, Huang Y, Zhu W, Zhou S, Zhou J, Zeng F, Liu X, Zhang Y and Yu J: An integrated analysis of miRNA and mRNA expressions in non-small cell lung cancers. *PLoS One* 6: e26502, 2011.
- Kumarswamy R, Mudduluru G, Ceppi P, Muppala S, Kozłowski M, Niklinski J, Papotti M and Allgayer H: MicroRNA-30a inhibits epithelial-to-mesenchymal transition by targeting Snail and is downregulated in non-small cell lung cancer. *Int J Cancer* 130: 2044-2053, 2012.
- Crawford M, Brawner E, Batte K, Yu L, Hunter MG, Otterson GA, Nuovo G, Marsh CB and Nana-Sinkam SP: MicroRNA-126 inhibits invasion in non-small cell lung carcinoma cell lines. *Biochem Biophys Res Commun* 373: 607-612, 2008.
- Xiong S, Zheng Y, Jiang P, Liu R, Liu X and Chu Y: MicroRNA-7 inhibits the growth of human non-small cell lung cancer A549 cells through targeting BCL-2. *Int J Biol Sci* 7: 805-814, 2011.
- Adams SJ, Aydin IT and Celebi JT: GAB2-a scaffolding protein in cancer. *Mol Cancer Res* 10: 1265-1270, 2012.
- Ding CB, Yu WN, Feng JH and Luo JM: Structure and function of Gab2 and its role in cancer (Review). *Mol Med Rep* 12: 4007-4014, 2015.
- Gu DH, Mao JH, Pan XD, Zhu H, Chen X, Zheng B and Shan Y: microRNA-302c-3p inhibits renal cell carcinoma cell proliferation by targeting Grb2-associated binding 2 (Gab2). *Oncotarget* 8: 26334-26343, 2017.
- Mu L, Guan B, Tian J, Li X, Long Q, Wang M, Wang W, She J, Li X, Wu D and Du Y: MicroRNA218 inhibits tumor angiogenesis of human renal cell carcinoma by targeting GAB2. *Oncol Rep* 44: 1961-1970, 2020.
- Yu S, Geng S and Hu Y: miR-486-5p inhibits cell proliferation and invasion through repressing GAB2 in non-small cell lung cancer. *Oncol Lett* 16: 3525-3530, 2018.
- Hu H, Tou FF, Mao WM, Xu YL, Jin H, Kuang YK, Han CB and Guo CY: microRNA-1321 and microRNA-7515 contribute to the progression of non-small cell lung cancer by targeting CDC20. *Kaohsiung J Med Sci* 38: 425-436, 2022.
- Ye J, Luo W, Luo L, Zhai L and Huang P: MicroRNA-671-5p inhibits cell proliferation, migration and invasion in non-small cell lung cancer by targeting MFAP3L. *Mol Med Rep* 25: 30, 2022.
- Shang Y, Zang A, Li J, Jia Y, Li X, Zhang L, Huo R, Yang J, Feng J, Ge K, *et al*: MicroRNA-383 is a tumor suppressor and potential prognostic biomarker in human non-small cell lung cancer. *Biomed Pharmacother* 83: 1175-1181, 2016.
- Zeng Y, Zhu J, Shen D, Qin H, Lei Z, Li W, Liu Z and Huang JA: MicroRNA-205 targets SMAD4 in non-small cell lung cancer and promotes lung cancer cell growth in vitro and in vivo. *Oncotarget* 8: 30817-30829, 2017.
- Qin Q, Wei F, Zhang J and Li B: miR-134 suppresses the migration and invasion of non-small cell lung cancer by targeting ITGB1. *Oncol Rep* 37: 823-830, 2017.
- Zhang JX, Zhai JF, Yang XT and Wang J: MicroRNA-132 inhibits migration, invasion and epithelial-mesenchymal transition by regulating TGF β 1/Smad2 in human non-small cell lung cancer. *Eur Rev Med Pharmacol Sci* 20: 3793-3801, 2016.
- Jiang W, He Y, Shi Y, Guo Z, Yang S, Wei K, Pan C, Xia Y and Chen Y: MicroRNA-1204 promotes cell proliferation by regulating PITX1 in non-small-cell lung cancer. *Cell Biol Int* 43: 253-264, 2019.
- Lu HM, Yi WW, Ma YS, Wu W, Yu F, Fan HW, Lv ZW, Yang HQ, Chang ZY, Zhang C, *et al*: Prognostic implications of decreased microRNA-101-3p expression in patients with non-small cell lung cancer. *Oncol Lett* 16: 7048-7056, 2018.
- Pang J, Dai L, Zhang C and Zhang Q: MiR-373 Inhibits the epithelial-mesenchymal transition of prostatic cancer via targeting runt-related transcription factor 2. *J Healthc Eng* 2021: 6974225, 2021.

39. Wu N, Liu X, Xu X, Fan X, Liu M, Li X, Zhong Q and Tang H: MicroRNA-373, a new regulator of protein phosphatase 6, functions as an oncogene in hepatocellular carcinoma. *FEBS J* 278: 2044-2054, 2011.
40. Voorhoeve PM, le Sage C, Schrier M, Gillis AJ, Stoop H, Nagel R, Liu YP, van Duijse J, Drost J, Griekspoor A, *et al*: A genetic screen implicates miRNA-372 and miRNA-373 as oncogenes in testicular germ cell tumors. *Adv Exp Med Biol* 604: 17-46, 2007.
41. Qu HW, Jin Y, Cui ZL and Jin XB: MicroRNA-373-3p inhibits prostate cancer progression by targeting AKT1. *Eur Rev Med Pharmacol Sci* 22: 6252-6259, 2018.
42. Ye Y, Zhang L, Song Y, Zhuang J, Wang G, Ni J, Zhang S and Xia W: MicroRNA373 exerts antitumor functions in human liver cancer by targeting Rab22a. *Mol Med Rep* 20: 3874-3882, 2019.
43. Yu MM, Wang GJ, Wu KH, Xue SL, Ju LL, Li QR, Xiong AW and Yin GP: MicroRNA-373-3p inhibits the growth of cervical cancer by targeting AKT1 both in vitro and in vivo. *Acta Biochim Pol* 68: 611-617, 2021.
44. Wang L, Qu J, Zhou L, Liao F and Wang J: MicroRNA-373 inhibits cell proliferation and invasion via targeting BRF2 in human non-small cell lung cancer A549 cell line. *Cancer Res Treat* 50: 936-949, 2018.
45. Wang Y, Xu Z and Wang X: miRNA-373 promotes urinary bladder cancer cell proliferation, migration and invasion through upregulating epidermal growth factor receptor. *Exp Ther Med* 17: 1190-1195, 2019.
46. Mu L, Guan B, Tian J, Li X, Long Q, Wang M, Wang W, She J, Li X, Wu D and Du Y: [Corrigendum] MicroRNA-218 inhibits tumor angiogenesis of human renal cell carcinoma by targeting GAB2. *Oncol Rep* 48: 191, 2022.
47. Zhuo Y, Li S, Hu W, Zhang Y, Shi Y, Zhang F, Zhang J, Wang J, Liao M, Chen J, *et al*: Targeting SNORA38B attenuates tumorigenesis and sensitizes immune checkpoint blockade in non-small cell lung cancer by remodeling the tumor microenvironment via regulation of GAB2/AKT/mTOR signaling pathway. *J Immunother Cancer* 10: e004113, 2022.
48. Horst B, Gruvberger-Saal SK, Hopkins BD, Bordone L, Yang Y, Chernoff KA, Uzoma I, Schwippen V, Liebau J, Nowak NJ, *et al*: Gab2-mediated signaling promotes melanoma metastasis. *Am J Pathol* 174: 1524-1533, 2009.
49. Bentires-Alj M, Gil SG, Chan R, Wang ZC, Wang Y, Imanaka N, Harris LN, Richardson A, Neel BG and Gu H: A role for the scaffolding adapter GAB2 in breast cancer. *Nat Med* 12: 114-121, 2006.
50. Xu LJ, Wang YC, Lan HW, Li J and Xia T: Grb2-associated binder-2 gene promotes migration of non-small cell lung cancer cells via Akt signaling pathway. *Am J Transl Res* 8: 1208-1217, 2016.
51. Zhang YM, Zhang ZQ, Liu YY, Zhou X, Shi XH, Jiang Q, Fan DL and Cao C: Requirement of Galphai1/3-Gab1 signaling complex for keratinocyte growth factor-induced PI3K-AKT-mTORC1 activation. *J Invest Dermatol* 135: 181-191, 2015.
52. Shioyama W, Nakaoka Y, Higuchi K, Minami T, Taniyama Y, Nishida K, Kidoya H, Sonobe T, Naito H, Arita Y, *et al*: Docking protein Gab1 is an essential component of postnatal angiogenesis after ischemia via HGF/c-met signaling. *Circ Res* 108: 664-675, 2011.
53. Jiang N, Dai Q, Su X, Fu J, Feng X and Peng J: Role of PI3K/AKT pathway in cancer: The framework of malignant behavior. *Mol Biol Rep* 47: 4587-4629, 2020.
54. Papadimitrakopoulou V: Development of PI3K/AKT/mTOR pathway inhibitors and their application in personalized therapy for non-small-cell lung cancer. *J Thorac Oncol* 7: 1315-1326, 2012.
55. Weng W, Liu C, Li G, Ruan Q, Li H, Lin N and Chen G: Long non-coding RNA SNHG16 functions as a tumor activator by sponging miR-3733p to regulate the TGF- β -R2/SMAD pathway in prostate cancer. *Mol Med Rep* 24: 843, 2021.
56. Wang L, Wang L, Chang W, Li Y and Wang L: MicroRNA-373 promotes the development of esophageal squamous cell carcinoma by targeting LATS2 and OXR1. *Int J Biol Markers* 34: 148-155, 2019.



Copyright © 2024 Zhu et al. This work is licensed under a Creative Commons Attribution-NonCommercial-NoDerivatives 4.0 International (CC BY-NC-ND 4.0) License.